Investigation of the Driver's Arm Viscoelastic Properties During Steering Vehicle Maneuver

Alaa Marouf, Philippe Pudlo, Chouki Sentouh, Mohamed Djemai

IEEE TRANSACTIONS ON SYSTEMS MAN AND CYBERNETICS: SYSTEMS 47-6 (2017) 1030-1036

Investigation of the Driver's Arm Viscoelastic Properties During Steering Vehicle Maneuver

Alaa Marouf, Philippe Pudlo, Chouki Sentouh, and Mohamed Djemaï

***Abstract*—Driver's arm viscoelastic properties during steering vehicle maneuver are very important information to understand how the driver regulates his torque and they could be used to design a new driver assistance system. This correspondence paper investigates the driver's arm viscoelastic properties during steering vehicle maneuver. First, a time-varying method for estimating driver's arm viscoelastic properties during driving the vehicle is proposed. Then, this method is implemented experimentally in order to examine the driver's arm viscoelastic properties during driving the vehicle. The estimation method does not require a specific perturbation torque to be applied during driving and could be applied online. The method is based on a time-varying model of the human driver's arm coupled with the electric power-assisted steering system model. Experiments were carried out with five healthy subjects who drove on a hardware-in-the-loop simulator without assistance and with assistance.**

I. Introduction

The assist torque in electric power-assisted steering (EPAS) systems is function of the driver torque. The driver torque could be expressed by a mechanical impedance properties (i.e., stiffness, viscosity, and inertia) [1]–[4]. These properties characterize the driver's arm movement and the interaction between the driver and the steering system, and could be used to provide an assistance based on the driver's arm properties. However, these properties are not measured. So, it should be estimated.

Generally, the human arm's impedance properties were identified using devices with electrical, hydraulic, or pneumatic actuators [2], [5]–[8]. The human subject was asked to track a virtual trajectory, a disturbance torque is applied by the actuator during the movement which leads to a new trajectory associated with the virtual trajectory by the impedance of the human arms. Then, the impedance properties are identified using the disturbance torque and the trajectory deviation. The disturbance torque should be designed properly to be used in the identification methods. It has been shown that the impedance depends on the activation level of muscles [9], the arm posture [5], [10], the speed of arm movement and load [11], the driving condition [12], and the muscle-contraction levels [13], [14].

For the identification process, several methods have been developed. Dolan *et al.* [2] estimated constant impedance components by using least mean square and three filtering methods to obtain the hand displacement derivatives. In [8], [13], and [15], a linear model with constant parameters for small motion was identified. The model is identified by applying small disturbance of short duration about the equilibrium position. The driver's neuromuscular system during steering vehicle is modeled by coefficients of stiffness, viscosity, and inertia [16]. The model parameters were identified by applying random perturbation torque and by measuring muscle activity using electromyography sensors. A nonparametric system identification algorithm was proposed in [17] to estimate endpoint stiffness from the relationship between the displacements and the forces required to perform these displacements, where continuous stochastic displacement perturbations were applied to the human arm during the movement. Estimating time-invariant neuromuscular admittance using frequency response functions was proposed in [18] and [19]. Bennett *et al.* [6] estimated time-varying properties by using so-called ensemble methods which relied on the autoregressive moving average model, repeated movement, and complicated procedure (e.g., chopping the data into single movement and aligning movement) to calculate the input–output of the model from the measurement of the joint angle and the applied disturbance torque. Xu and Hollerbach [7] proposed a method for estimating time-varying impedance parameters. The method is based on the standard least square, the procedure proposed by Bennett *et al*. [6], low-pass filter to obtain the derivatives of the joint angle, and high-pass filter to separate the voluntary movement and the perturbed movement. Mulder *et al.* [20] used a model of neuromuscular system to generate times-variant data, then the Morlet wavelet analysis was used to identify the time variant neuromuscular admittance model. The proposed method requires a force perturbation signal, and estimating the variation of each of the admittance properties is not discussed.

The existing methods consider either constant or variables properties. The methods that consider constant properties are valid for small disturbance torque (i.e., fixed position) and they cannot estimate the changes in the human arm properties. The methods that consider time-varying properties required disturbance torque to be applied during the movement, and use a complicated procedure to compute the average movement and the derivatives of the arm movement. The influence of using disturbance torque and averaging movement (i.e., aligning and shifting the data) on the resolution of these methods is not studied. Furthermore, the use of low-pass filters to calculate the derivatives of the arm movement leads to a big error in the identified parameters when the position or speed are constant or small.

In [21], a preliminary study on an identification method to estimate the impedance properties was presented. In this correspondence paper, we extend our previous work to validate the identification method under different conditions and with several subjects, to examine the time-varying changes in the driver's arm viscoelastic properties during driving the vehicle, to see how the driver regulates

This work was supported in part by the International Campus on Safety and Intermodality in Transportation, in part by the European Community, in part by the Regional Delegation for Research and Technology, in part by the Ministry of Higher Education and Research, in part by the Nord/Pas-de-Calais Region, and in part by the National Center for Scientific Research. This paper was recommended by Associate Editor B.-F. Wu.

The authors are with the University of Lille Nord de France, University of Valenciennes and Hainaut-Cambrésis, Laboratory of Automation Control, Mechanical Engineering, Computer Science, Industrial and Human, French National Center for Scientific Research (CNRS), UMR 8201, Campus du Mont Houy, F-59313 Valenciennes, France (e-mail: alaa.marouf@gmail.com; philippe.pudlo@univ-valenciennes.fr; chouki.sentouh@univ-valenciennes.fr; mohamed.djemai@univ-valenciennes.fr).

DOI : 10.1109/TSMC.2016.2523915

TABLE I
NOMENCLATURE DEFINITIONS

Symbol	Description
$\theta_c, \ddot{\theta}_c$	steering wheel speed and acceleration
$\dot{\theta}_m, \ddot{\theta}_m$	motor speed and acceleration
J_c	steering column moment of inertia
B_c	steering column viscous damping
K_c	steering column stiffness
M_r	mass of the rack
B_r	viscous damping of the rack
R_p	steering column pinion radius
K_r	tire spring rate
J_m	motor moment of inertia
B_m	motor shaft viscous damping
N	motor gear ratio

his properties, and to see how the assistance influences the driver's viscoelastic properties. For these objectives, we perform experiments with five subjects who drove on a hardware-in-the-loop (HIL) simulator without and with assistance. The identification method does not require a specific disturbance torque to be applied during the movement which may be disturb the driver during voluntary steering maneuver. The viscoelastic properties are estimated from the driver torque and not from the disturbance torque which leads to improve the temporal resolution of the identified parameters.

The remainder of this paper is organized as follows. Section II formalizes the problem and presents a solution to identify online the driver's arm viscoelastic properties during driving the vehicle. Section III describes the HIL simulator and reports the experimental results. Finally, in Section IV, the conclusion is drawn. Nomenclature definitions are provided in Table I.

II. DRIVER'S ARM VISCOELASTIC PROPERTIES ESTIMATION METHOD

In this section, we recall an identification algorithm for online time-varying system. We propose a model that combines the driver's arm and the EPAS system, then we construct the regression model from the proposed model for the application of the identification algorithm, and finally we estimate the input–output of the regression model so that the identification algorithm could be applied to identify the driver's arm properties.

A. Online Estimation Algorithm

The problem of designing identification algorithms for linear time-varying systems has been addressed in many works [22]–[24]. The exponentially weighted recursive least squares (EWRLSs) algorithm is selected for its good convergence and its capability to track the parameters [22]–[24]. The EWRLS can be applied to the so-called linear regression model

$$T(t) = \Theta^T(t)Z(t) \tag{1}$$

where T is the measured output variable, Θ is the regressor vector which contains the measured variables, and Z is the vector of unknown functions.

The EWRLS aims to identify the vector of unknown functions $Z(t)$ by using the measured input–output data $[\Theta(t), T(t)]$. The EWRLS solution $\hat{Z}(t)$ to the system (1) which minimizes the cost function

$$J = \int_0^t \lambda^{t-\tau}\Big(T(\tau) - \hat{T}(\tau)\Big)^2 d\tau, \quad \hat{T}(\tau) = \Theta^T(\tau)\hat{Z}(\tau)$$

is given by [22]–[24]

$$\begin{cases} \dot{\hat{Z}}(t) = P(t)\Theta(t)\Big(T(t) - \Theta^T(t)\hat{Z}(t)\Big) \\ \dot{P}(t) = -P(t)\Theta(t)\Theta^T P(t) + \lambda P(t) \end{cases} \tag{2}$$

where $\hat{Z}$ is the identified vector, λ is a weighted factor, and $\hat{T}$ is the predicted output.

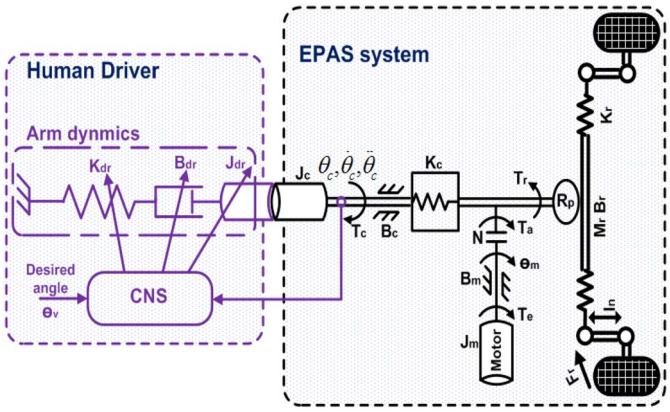

Fig. 1. Driver's arm and EPAS model.

TABLE II
R^2 OF THE FITTED MODELS WITH AND WITHOUT ASSISTANCE

Sub/R^2	Model wna with Tg	Model wna without Tg	Model wa with Tg	Model wa without Tg
Subject1	88%	63%	78%	49%
Subject2	87%	63%	82%	51%
Subject3	89%	60%	79%	45%
Subject4	92%	75%	89%	52%
Subject5	89%	69%	83%	48%

B. Model-Based Estimation

First, a model that describes the dynamic of the driver's arm while driving the vehicle is required. In order to estimate the variations in the driver's viscoelastic properties during driving, we consider time varying stiffness, viscosity, and inertia as shown in Fig. 1. The model could be explained as: to achieve a desired trajectory, the central nervous system treats the information come from the environment (e.g., desired angle, steering torque feedback, and road conditions) and regulates the viscoelastic properties of the arms (i.e., arm impedance) to make the proper steering angle. In turning the steering wheel, the driver generates torque which acts through the driver's arm admittance and results in a steering angle. The motion law that describes the movement

$$\begin{cases} (J_c + J_{\rm dr}(t))\ddot{\theta}_c = -(B_c + B_{\rm dr}(t))\dot{\theta}_c \\ \qquad\qquad -(K_c + K_{\rm dr}(t))\theta_c + \frac{K_c}{N}\theta_m \\ J_{\rm eq}\ddot{\theta}_m = \frac{K_c}{N}\theta_c - \left(\frac{K_c + R_p^2 K_r}{N^2}\right)\theta_m - B_{\rm eq}\dot{\theta}_m + T_e - \frac{T_r}{N} \end{cases} \tag{3}$$

where $J_{\rm eq} = J_m + (R_p^2/N^2)M_r$, $B_{\rm eq} = B_m + (R_p^2/N^2)B_r$, and $\theta_m = (Nx_r/R_p)$. θ_c, θ_m, and x_r are, respectively, the steering wheel angle, the motor's angular position, and the rack position; T_e is the electromagnetic torque generated by the motor; $T_a = NT_e$ is the assistance torque; T_r is the road reaction torque; and $J_{\rm dr}(t)$, $B_{\rm dr}(t)$, and $K_{\rm dr}(t)$ represent driver's arm inertia, viscosity, and the stiffness. Table II defines the other EPAS model parameters. The parameters (J_c, B_c, K_c, $J_{\rm eq}$, $B_{\rm eq}$, K_r, and N) of the EPAS dynamics are known. These parameters could be identified when the driver does not hold the steering wheel (i.e., the steering wheel is free) [25], which allows to separate between the EPAS dynamics and the driver's arm dynamics. The objective is to identify the driver's arms properties $[K_{\rm dr}(t), B_{\rm dr}(t)$, and $J_{\rm dr}(t)]$. Let us define the unknown driver's arms properties as

$$T_{\rm dr}(t) = J_{\rm dr}(t)\ddot{\theta}_c(t) + B_{\rm dr}(t)\dot{\theta}_c(t) + K_{\rm dr}(t)\theta_c(t). \tag{4}$$

Using (4), (3) takes the following state-space form:

$$\begin{cases} \dot{x}(t) = Ax(t) + B_u u(t) + B_w w(t) \\ y(t) = Cx(t) = \begin{bmatrix} \theta_c & \theta_m \end{bmatrix}^T \end{cases} \tag{5}$$

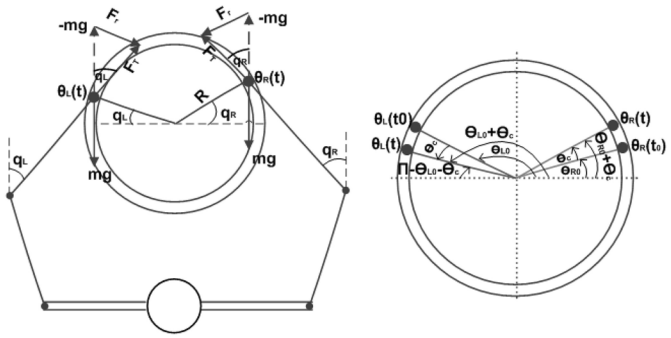

Fig. 2. Gravity torque representation. (a) Gravity force of the two arms. (b) Position of the two hands on the steering wheel.

where $x = \left[\theta_c\ \dot{\theta}_c\ \theta_m\ \dot{\theta}_m\right]^T$ is the state vector; $u = T_e$ is the known input; $w = \left[T_{\rm dr}\ T_r\right]^T$ represents the vector of unknown inputs which is composed of driver torque $T_{\rm dr}$ and road reaction torque T_r; and y is the measurement signal. Our objective is to identify the driver's arms properties by measuring $y(t)$. By estimating ($\dot{\theta}_c$, $\ddot{\theta}_c$, $T_{\rm dr}$) and using (4), we can construct the following regression model:

$$T_{\rm dre}(t) = \Theta_e^T(t) Z(t) \tag{6}$$

where $T_{\rm dre}(t)$ is the estimated driver torque (i.e., the model output), $\Theta_e^T(t) = \left[\theta_c(t) \quad \hat{\dot{\theta}}_c(t) \quad \hat{\ddot{\theta}}_c(t)\right]$ is the estimated regressor vector, and $Z(t) = \left[K_{\rm dr}(t) \quad B_{\rm dr}(t) \quad J_{\rm dr}(t)\right]^T$ is the vector of unknown properties to be identified.

So, the solution of our problem is to design an observer to estimate ($T_{\rm dre}$, Θ_e), and then use an identification algorithm to identify the vector $Z(t)$. Using the EPAS dynamic model (5) and the sliding mode observer with unknown inputs in conjunction with second-order sliding mode differentiators [21], [26], the vector $\Theta_e(t)$ and $T_{\rm dre}(t)$ could be estimated. Then, using the regression model (6) and the EWRLS algorithm (2), the vector $Z(t)$ could be identified.

In addition to the muscular torque $T_{\rm dr}$, the gravity torque acts on the steering wheel. The gravity torque T_g is due to the weight of arms, and resulting from the tangential component of the gravity force, while the radial component does not contribute to the rotation of the steering wheel (see Fig. 2). The gravity torque depends on the angles of the two arms

$$T_g = T_{gR} + T_{gL} = -mgRl\cos\phi\left[\cos q_R - \cos q_L\right]$$

where m is the mass of the arm; l is the forearm length; R is the radius of the steering wheel; g is the gravitational acceleration; θ_{R0} and θ_{L0} are, respectively, the initial positions of the right and left hand on the steering wheel; $\theta_R = \theta_{R0} + \theta_c$ and $\theta_L = \theta_{L0} + \theta_c$ are, respectively, the angles of the right and left hands on the steering wheel; and ϕ is the inclination of the steering wheel with respect to the vertical axis. Assuming that the driver holds the steering wheel with both hands around the initial position "nine-to-three" (i.e., our experiments) and follows the desired trajectory without releasing the steering wheel ($\theta_{R0} = \varepsilon_R$, $\theta_{L0} = \pi - \varepsilon_L$) and ($q_R = \theta_c + \varepsilon_R$, $q_L = \pm(\theta_c - \varepsilon_L)$), then the gravity torque is given by:

$$T_g \approx mgRl\cos\phi(\varepsilon_R + \varepsilon_L)\sin\theta_c = F_g(t)\sin\theta_c(t). \tag{7}$$

Under this consideration, the total driver's exerted torque can be defined as

$$T_{\rm dr}(t) = J_{\rm dr}(t)\ddot{\theta}_c(t) + B_{\rm dr}(t)\dot{\theta}_c(t) + K_{\rm dr}(t)\theta_c(t) + F_g\sin\theta_c. \tag{8}$$

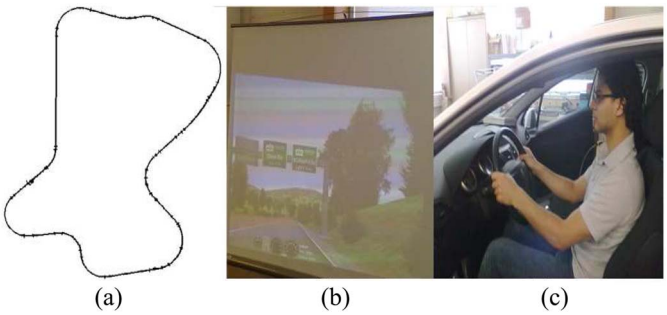

Fig. 3. (a) Test track. (b) Driving course and examples of the presentation screen. (c) Driver holding the steering wheel.

With this representation, the regressor vector becomes $\Theta_e^T = \left[\theta_c(t) \quad \hat{\dot{\theta}}_c(t) \quad \hat{\ddot{\theta}}_c(t) \quad \sin\theta_c(t)\right]$ and the unknown vector becomes $Z = \left[K_{\rm dr}(t) \quad B_{\rm dr}(t) \quad J_{\rm dr}(t) \quad F_g(t)\right]^T$.

III. Experimental Results

The aim of the experiments is to validate the identification method, to examine the viscoelastic properties of the driver's arm during vehicle steering maneuver, and to see how the assistance would influence the driver's arm viscoelastic properties. Five healthy subjects, male Ph.D. students, participated in the experiments. The experiments were performed using an HIL simulator developed at LAMIH laboratory. The developed HIL is composed of the EPAS system, the reaction force system, and the SCANeR studio system. The three systems are embedded inside an actual Peugeot 207 vehicle. The EPAS system is the real existing system in a production vehicle equipped with EPAS provided by JTEKT Corporation. The reaction force system load the road reaction force on the rack. The target road reaction force are received from the SCANeR studio system (e.g., vehicle model), then a control algorithm is applied to load this force on the rack. The SCANeR system generates also 3-D driving environment (e.g., road, decoration, and traffic). The assist motor and the road reaction motor are controlled by MicroAutoBox 1401/1505 driven by computer-MATLAB/Simulink. The sampling time is 0.0001 s. The assist motor angle, the steering wheel angle, the steering torque, and the reaction force applied on the rack are measured. The steering wheel angle is measured using two turn potentiometer, the motor angle is measured using resolver, and the steering torque is measured using rotation torque sensor (TR602, maximum torque: 20 Nm). The measured signals are transformed into digital signals using 12 bit analog-to-digital converter. The accuracy of the potentiometer is ($\Delta\theta_c = 720°/4095 = \pm 0.1758° = \pm 0.003$ rad). The accuracy of the resolver ($\Delta\theta_m = 360°/4095 = \pm 0.0879° = \pm 0.0015$rad). The accuracy of torque sensor is ($\Delta T_c = 20/4095 = \pm 0.0048$Nm). Subjects were asked to be seated in an adjustable car, to hold the steering wheel with both hands around the position "nine-to-three" [see Fig. 3(c)], to maintain central lane position as much as possible without releasing the steering wheel, and to fix their speed around 15 m/s (see Fig. 3).

A. Model Validation

Figs. 4 and 5 show the driver's inputs to the steering wheel while driving on the track in the two cases, without assistance wna and with assistance wa. As can be seen in Fig. 4(a) that the driver performs approximately the same steering angle (i.e., same trajectory). However, the driver provides less torque with assistance [Fig. 4(b)]. It can be seen in Fig. 4(b) and (c) that the driver torque and the road reaction torque could be estimated with good accuracy. The speed and the acceleration are not measured. To demonstrate the effectiveness of the observer, we compare the online estimated velocity

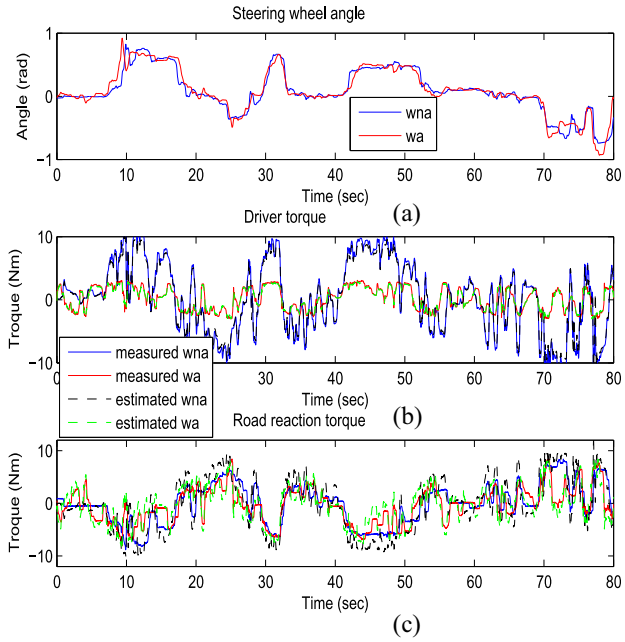

Fig. 4. Driver torque and road reaction torque during driving. (a) Steering angle without assistance "wna" and with assistance "wa." (b) Measured and estimated driver torque without assistance wna and with assistance wa. (c) Measured and estimated road reaction torque without assistance wna and with assistance wa.

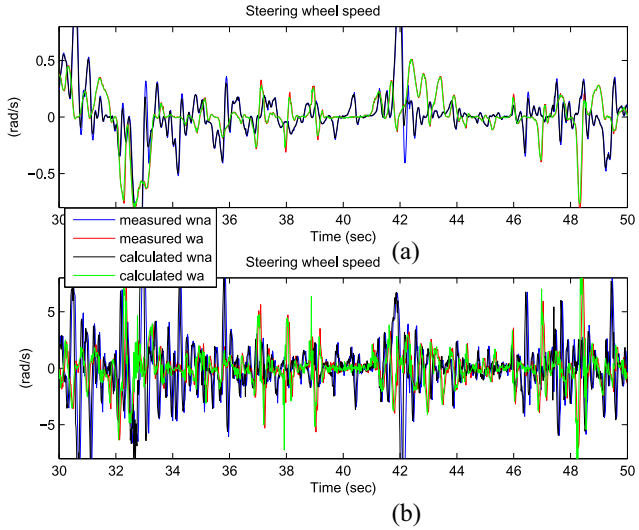

Fig. 5. Speed and acceleration estimation. (a) Speed. (b) Acceleration.

and acceleration with the velocity and acceleration calculated using MATLAB functions "calculated." First, the function "filtfilt," performs zero-phase filtering, is applied to the measured angles in order to reduce the noise and filter delay, and then the function "diff" is applied to the filtered signal to obtain the derivatives. As shown in Fig. 5(a) and (b), both velocity and acceleration from observer are close to the calculated signals.

Fig. 6(a) and (b) shows the estimated driver torque (T_{dre}), the identified driver torque ($\hat{T}_{\mathrm{dre}}$) predicted by the model without considering gravity torque (4), and the torque predicted by the model with considering gravity torque (8). It can be seen that the prediction capacity of the model with gravity torque is better than the model without gravity torque. To evaluate the quality of the identified model, we calculate the square of the correlation between the estimated driver torque and

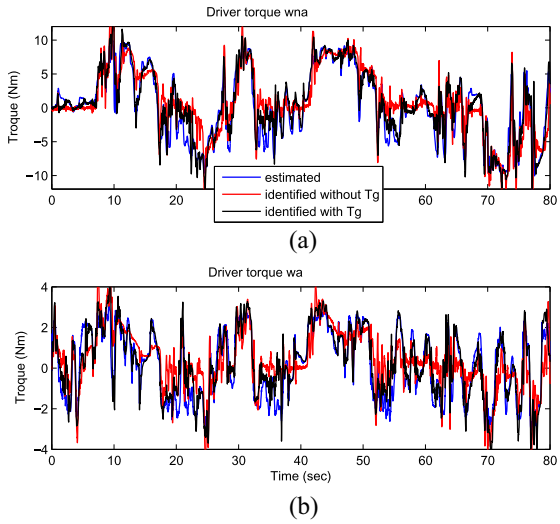

Fig. 6. Identified driver torque versus estimated driver torque for a typical subject. (a) Without assistance wna. (b) With assistance wa.

the identified driver torque (i.e., R^2 or coefficient of determination), which is defined as

$$R^2 = 1 - \frac{\sum_i \left(T_{\mathrm{de}}(i) - \hat{T}_{\mathrm{de}}(i)\right)^2}{\sum_i \left(T_{\mathrm{de}}(i) - \mathrm{mean}(T_{\mathrm{de}})\right)^2}.$$

Table II shows the R^2 value of the fitted models with and without considering the gravity torque for the five subjects while driving without and with assistance.

As seen in Table II, the prediction capacity (i.e., R^2) of the model with considering the gravity torque is better than the model without considering the gravity torque when driving with and without assistance. The predicted torque deviates much from the original torque when the amplitude of the steering wheel angle, speed, and acceleration is small. In fact, the inputs of the model without gravity torque in this case does not contain significant information. Also, we note that the value of the R^2 for the two models is smaller with assistance than without assistance. This could be due to the fact that the model without assistance is more rich in information than with assistance (e.g., amplitude of the driver torque).

B. Viscoelastic Properties Without and With Assistance

We present here the identified properties by the two models for a typical subject while driving without and with assistance.

Fig. 7(a) and (b) shows the stiffness identified by the models without and with gravity torque while driving without and with assistance. We observe in Fig. 7(a) that the stiffness varies with the time, the value of the stiffness with assistance is smaller than without assistance, the shape of the stiffness variation with assistance is similar to this one without assistance, and the amplitude of the variation of the stiffness is smaller with assistance than without assistance. It could be explained that the assistance make the driver regulate his stiffness better than without assistance.

We can see in Fig. 7(a) and (b) that the amplitude of the stiffness identified by the model with gravity is higher than the stiffness identified by the model without gravity. This could be explained by that the driver control his stiffness to resist the gravity force [see Fig. 7(c)] and maintain the steering wheel. As can be seen in Fig. 7(c), the gravity force with assistance is smaller than without assistance ($-F_g \approx 100$, wna, $-F_g \approx 86$, wa), there is a peak in F_g when the driver changes the direction of the steering wheel, and this

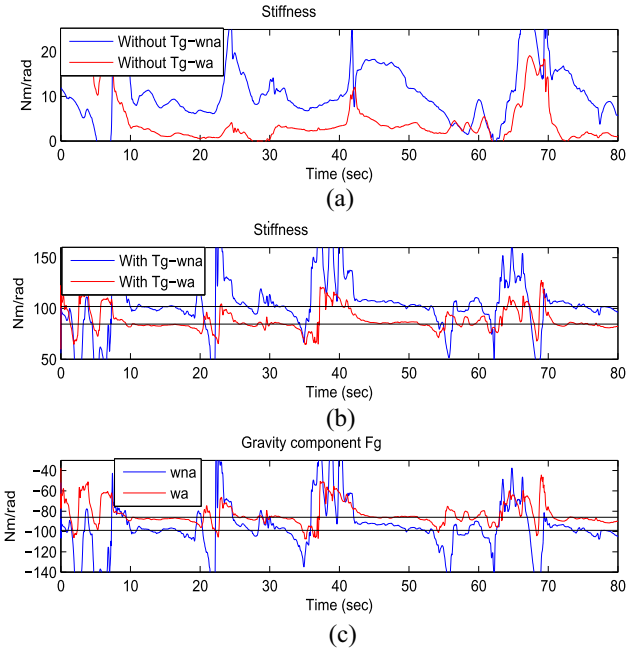

Fig. 7. Identified stiffness and gravity component. Stiffness identified by the model (a) without gravity and (b) with gravity. (c) Gravity component Fg.

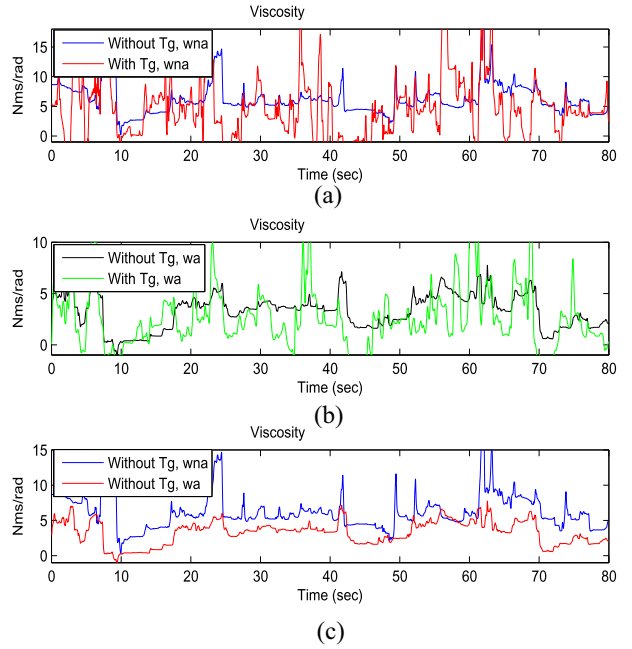

Fig. 8. Identified viscosity. (a) Model without and with gravity—without assistance. (b) Model without and with gravity—with assistance. (c) Model without gravity—without and with assistance.

peak is larger in the case without assistance. The mean value of the two values of F_g, wna and wa, is approximately -93 and the relative error is 0.08. The difference between the two values could be an estimation error, or due to the small difference in the performed steering angle in the two cases, or due to the fact that the driver is more relaxed when he drives with assistance which affects the muscular contraction and the musculoskeletal tensions.

Fig. 8(a) and (b) shows the viscosity identified by the two models, without Tg and with Tg, when driving without and with assistance. It could be seen that the form of variation of viscosity identified by

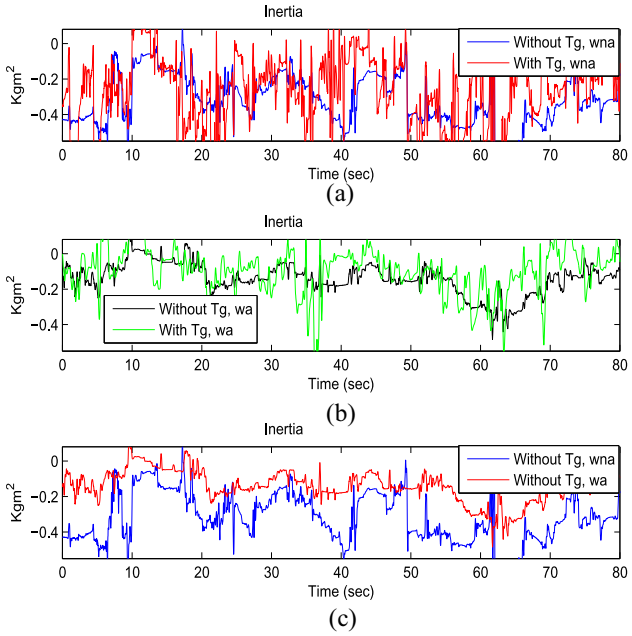

Fig. 9. Identified inertia. (a) Model without and with gravity—without assistance. (b) Model without and with gravity—with assistance. (c) Model without gravity—without and with assistance.

the model without gravity differs from that identified by the model with gravity when the torque predicted by this model deviates from the original torque, and the amplitude of variation is greater with the model with gravity. We observe from Fig. 8(c) that the form of variation of viscosity with assistance is similar to this without assistance. However, the value and the amplitude of the variation of the viscosity with assistance are smaller than without assistance.

Fig. 9(a) and (b) shows the inertia identified by the two models, without T_g and with T_g, when driving without and with assistance. The negative sign of inertia, hypothetical sign, means that the inertia torque will opposite the direction of the applied torque. One can see that the form of variation of the inertia identified by the two models are similar. However, the amplitude of variation is greater with the model with gravity. As be shown in Fig. 9(c), the driver reduces his inertia when driving with assistance.

We can notice that the driver's arms viscoelastic properties vary according to the driver's efforts. When the driver reduces his efforts, the value of these properties decreases, and the amplitude of its variation decreases also, however, without significant changes in its pattern. We observe that the contribution of stiffness in the torque response is important when the driver reaches the desired position and holds the steering wheel (i.e., straight line), and the contribution of the viscosity is important when the driver changes the direction of the movement (i.e., lane change maneuvre).

We assessed the natural frequency and the damping ratio, Fig. 10(a) and (b), defined for a second-order system (e.g., model without T_g) as $F_n = (1/2\pi)\sqrt{K_{\rm dr}/J_{\rm dr}}$ and $\xi = B_{\rm dr}/\sqrt{4K_{\rm dr}J_{\rm dr}}$.

It could be seen that the natural frequency varies according to the steering condition, and the pattern of its variation without assistance is similar to this one with assistance. The average values without and with assistance are, respectively, 0.96, and 0.76 Hz. The natural frequency of the subject decreases as the magnitude of his torque decreases. We observe that the damping ratio with assistance is bigger than without assistance. This indicates that the damping is more important in the case with assistance (i.e., minimum effort). It could be seen that the damping ratio is almost bigger than one which indicates that human arms are over damping.

DOI : 10.1109/TSMC.2016.2523915

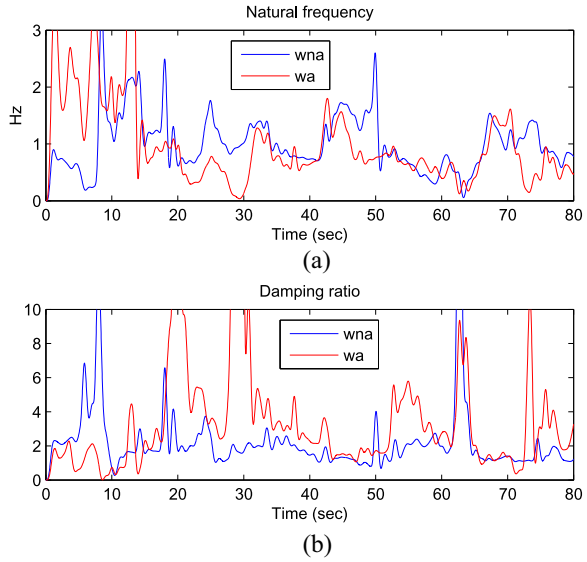

Fig. 10. Estimated natural frequency and damping ratio. (a) Natural frequency. (b) Damping ratio.

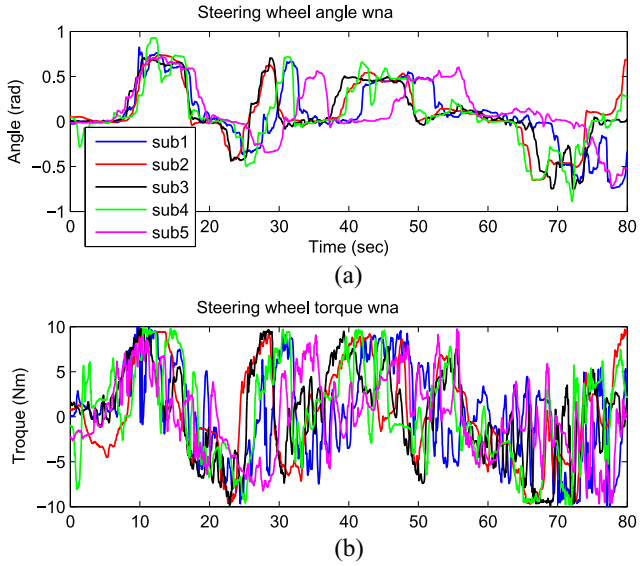

Fig. 11. Time histories of the steering wheel angle and the driver torque for five subjects without assistance. (a) Steering angle. (b) Driver torque.

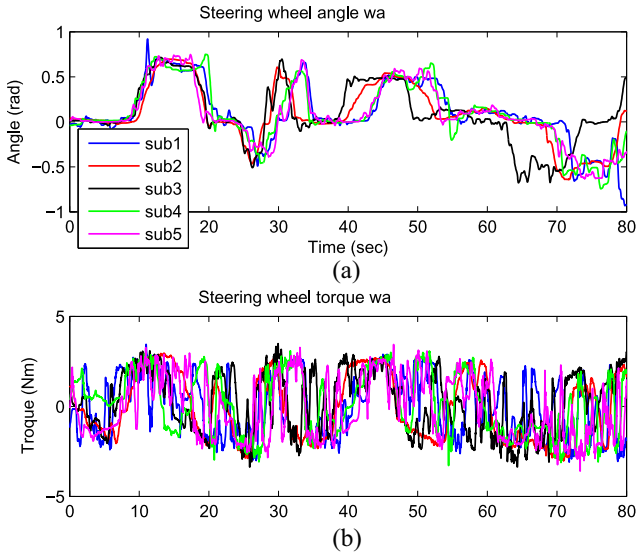

Fig. 12. Time histories of the steering wheel angle and the driver torque for five subjects with assistance. (a) Steering angle. (b) Driver torque.

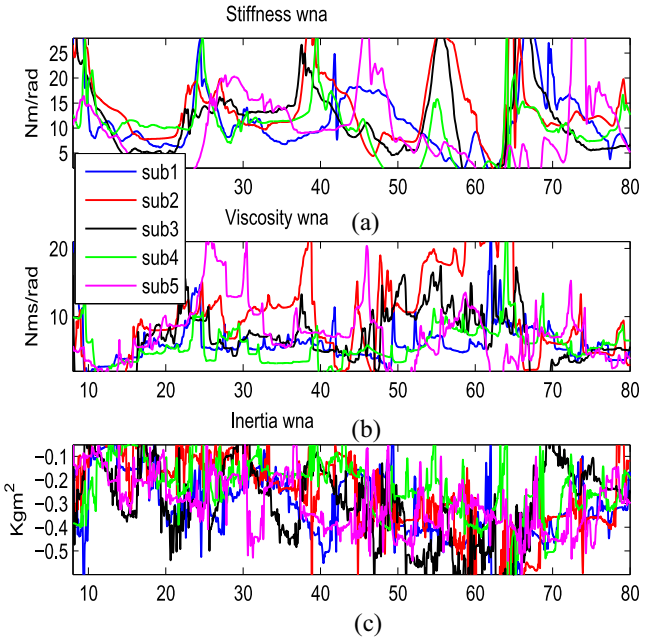

Fig. 13. Identified properties of five subjects when driving without assistance. (a) Stiffness. (b) Viscosity. (c) Inertia.

C. Subjects Comparison

We aim to know if we can distinguish between the subjects using their viscoelastic properties in order to develop an assistance adapted to the people's viscoelastic properties. For this purpose, we compare the identified viscoelastic properties of the subjects. Figs. 11 and 12 show the provided steering wheel angle and driver torque for five subjects when driving without and with assistance. As can be seen from these figures that the subjects do not perform exactly the same steering wheel angle (e.g., the same trajectory), there is delay between the performed steering angle due to the different driving styles. We can see in Fig. 11(a) that subjects 2 and 3 perform approximately the same steering angle, and the subjects 2–4 perform approximately the same steering angle between 32 and 100 s. We observe in Fig. 12(a) that subjects 2 and 3 perform approximately the same steering angle between 0 and 40 s, and subjects 1 and 4 effect approximately the same steering angle between 0 and 68 s. We remark that the pattern of the torque provided by the subjects may be differ slightly even when the subjects perform the same steering angle.

Figs. 13 and 14 show, respectively, comparison between the viscoelastic properties of five subjects when driving without assistance and with assistance. As can be seen in Figs. 13(a) and 14(a), there are differences between the subjects in average value and in amplitude of the variation of the stiffness. This difference could be due to the fact that subjects do not perform exactly the same steering angle and provide exactly the same torque. Regarding the viscosity [Figs. 13(b) and 14(b)], we can remark that the viscosity of subjects 2 and 3 are considerably different, when driving without assistance and with assistance, even when both subjects perform the same maneuvers [see Figs. 11(a) and 12(a)]. We can see also that there is a different in value of the viscosity between the subjects. As can be seen in Figs. 13(c) and 14(c), the pattern of the identified

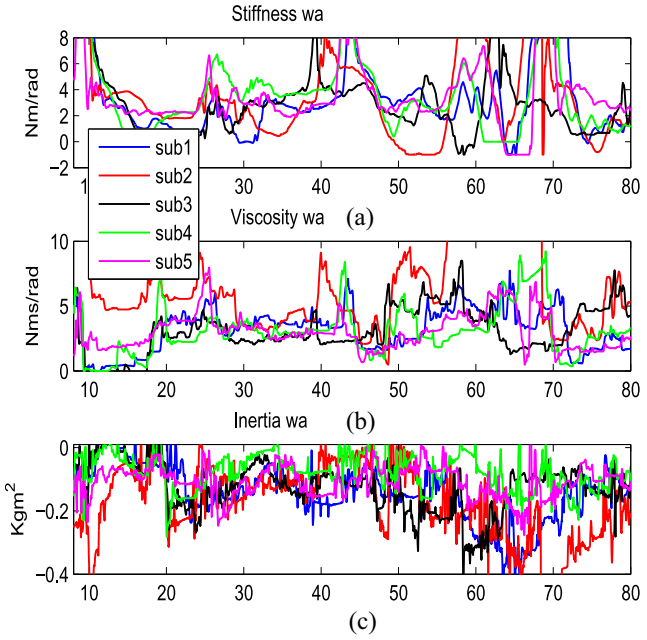

Fig. 14. Identified properties of five subjects when driving with assistance. (a) Stiffness. (b) Viscosity. (c) Inertia.

inertia is similar for all subjects. There are differences in the average value and in the amplitude of the variation. We can conclude that the driver's viscoelastic during steering maneuver are different. These differences could be due to the musculoskeletal characteristics of each driver and to the driver's style of driving.

IV. Conclusion

In this correspondence paper, an online method for estimating driver's arm viscoelastic properties during driving vehicle was proposed. The method is designed using sliding mode observer and EWRLS algorithm based on a time-varying model of driver's arm in interaction with EPAS system. The method does not require perturbation torque which may influence the driver behavior. Experiments were carried out to validate the identification method and to examine the viscoelastic properties during driving vehicle. The experimental results show that the proposed model can predict the torque provided by driver during steering the vehicle, which confirms the validity of both the model and the identification method. It has been indicated that the driver adapts his arm properties during steering vehicle depending on steering condition, the value of the viscoelastic properties, and the amplitude of its variation decrease without significant changes in its pattern when the driver reduces his effort. It is indicated that the damping is more important when the driver reduces his torque and the driver's natural frequency decreases when the driver reduces his torque. Finally, the results showed that the driver's viscoelastic properties during steering maneuver may differ due to the driving styles and to the musculoskeletal characteristics. In the future work, the design of an assistance for the EPAS system based on driver's viscoelastic properties will be developed.

References

[1] T. Flash, "The control of hand equilibrium trajectories in multi-joint arm movements," *Biol. Cybern.*, vol. 57, nos. 4–5, pp. 257–274, 1987.

[2] J. M. Dolan, M. B. Friedman, and M. L. Nagurka, "Dynamic and loaded impedance components in the maintenance of human arm posture," *IEEE Trans. Syst., Man, Cybern.*, vol. 23, no. 3, pp. 698–709, May/Jun. 1993.

[3] K. P. Tee, E. Burdet, C. M. Chew, and T. E. Milner, "A model of force and impedance in human arm movements," *Biol. Cybern.*, vol. 90, no. 5, pp. 368–375, 2004.

[4] T. Tsuji and Y. Tanaka, "Tracking control properties of human-robotic systems based on impedance control," *IEEE Trans. Syst., Man, Cybern. A, Syst., Humans*, vol. 35, no. 4, pp. 523–535, Jul. 2005.

[5] F. A. Mussa-Ivaldi, N. Hogan, and E. Bizzi, "Neural, mechanical, and geometric factors subserving arm posture in humans," *J. Neurosci.*, vol. 5, no. 10, pp. 2732–2743, 1985.

[6] D. J. Bennett, J. M. Hollerbach, Y. Xu, and I. W. Hunter, "Time-varying stiffness of human elbow joint during cyclic voluntary movement," *Exp. Brain Res.*, vol. 88, no. 2, pp. 433–442, 1992.

[7] Y. Xu and J. M. Hollerbach, "A robust ensemble data method for identification of human joint mechanical properties during movement," *IEEE Trans. Biomed. Eng.*, vol. 46, no. 4, pp. 409–419, Apr. 1999.

[8] Y. Kashiba, Y. Tanaka, T. Tsuji, N. Yamada, and T. Suetomi, "Analysis of human hand impedance properties depending on driving conditions," in *Proc. 5th Int. Workshop Comput. Intell. Appl.*, Playa del Carmen, Mexico, 2009, pp. 88–93.

[9] S. C. Cannon and G. I. Zahalak, "The mechanical behavior of active human skeletal muscle in small oscillations," *J. Biomech.*, vol. 15, no. 2, pp. 111–121, 1982.

[10] T. Tsuji, P. G. Morasso, K. Goto, and K. Ito, "Human hand impedance characteristics during maintained posture," *Biol. Cybern.*, vol. 72, no. 6, pp. 475–485, 1995.

[11] T. E. Milner, "Dependence of elbow viscoelastic behavior on speed and loading in voluntary movements," *Exp. Brain Res.*, vol. 93, no. 1, pp. 177–180, 1993.

[12] D. I. Katzourakis, D. A. Abbink, E. Velenis, E. Holweg, and R. Happee, "Driver's arms' time-variant neuromuscular admittance during real car test-track driving," *IEEE Trans. Instrum. Meas.*, vol. 63, no. 1, pp. 221–230, Jan. 2014.

[13] T. Tsuji and M. Kaneko, "Estimation and modeling of human hand impedance during isometric muscle contraction," in *Proc. ASME Dyn. Syst. Control Div.*, vol. 58. Atlanta, GA, USA, 1996, pp. 575–582.

[14] H. Gomi and R. Osu, "Task-dependent viscoelasticity of human multijoint arm and its spatial characteristics for interaction with environments," *J. Neurosci.*, vol. 18, no. 21, pp. 8965–8978, 1998.

[15] Y. Tanaka *et al.*, "Analysis and modeling of human impedance properties for designing a human-machine control system," in *Proc. IEEE Int. Conf. Robot. Autom.*, Rome, Italy, 2007, pp. 3627–3632.

[16] A. Pick and D. J. Cole, "Neuromuscular dynamics and the vehicle steering task," in *Proc. 18th IAVSD Symp. Veh. Syst. Dyn.*, vol. 5. 2003, pp. 2732–2743.

[17] E. J. Perreault, R. F. Kirsch, and P. E. Crago, "Effects of voluntary force generation on the elastic components of endpoint stiffness," *Exp. Brain Res*, vol. 141, no. 3, pp. 312–323, 2001.

[18] F. C. T. van der Helm, A. C. Schouten, E. de Vlugt, and G. G. Brouwn, "Identification of intrinsic and reflexive components of human arm dynamics during postural control," *J. Neurosci. Methods*, vol. 119, no. 1, pp. 1–14, 2002.

[19] D. A. Abbink, M. Mulder, F. C. van der Helm, M. Mulder, and E. R. Boer, "Measuring neuromuscular control dynamics during car following with continuous haptic feedback," *IEEE Trans. Syst., Man, Cybern. B, Cybern.*, vol. 41, no. 5, pp. 1239–1249, Oct. 2011.

[20] M. Mulder *et al.*, "Identification of time variant neuromuscular admittance using wavelets," in *Proc. IEEE Int. Conf. SMC*, Anchorage, AK, USA, 2011, pp. 1474–1480.

[21] A. Marouf, P. Pudlo, C. Sentouh, and M. Djemai, "Identification of human arm viscoelastic properties during vehicle steering maneuver," in *Proc. IEEE Conf. SMC*, San Diego, CA, USA, 2014, pp. 3342–3347.

[22] L. Ljung and T. Söderström, *Theory and Practice of Recursive Identification*. Cambridge, MA, USA: MIT Press, 1983.

[23] G. C. Goodwin and K. S. Sin, *Adaptive Filtering Prediction and Control*. Englewood Cliffs, NJ, USA: Prentice-Hall, 1984.

[24] S. Sastry and M. Bodson, *Adaptive Control: Stability, Convergence, and Robustnessr*. Englewood Cliffs, NJ, USA: Prentice-Hall, 1987.

[25] A. Marouf, "Contribution á la commande du système de direction assistée electrique," Ph.D. dissertation, LAMIH Lab., Univ. Valenciennes and Hainaut-Cambrésis, Valenciennes, France, 2013.

[26] A. Marouf, M. Djemai, C. Sentouh, and P. Pudlo, "A new control strategy of an electric-power-assisted steering system," *IEEE Trans. Veh. Technol.*, vol. 61, no. 8, pp. 3574–3589, Oct. 2012.